

# COMPASS experiment at CERN: open charm results and future hadron program

O.Kouznnetsov<sup>a</sup>

<sup>a</sup>CEA-Saclay Service de Physique Nucleaire, F-91191 Gif-sur-Yvette, France *and*  
Joint Institute of Nuclear Research, Joliot Curie 6, 141980 Dubna, Russia

## On behalf of the COMPASS collaboration

COMPASS (COmmon Muon and Proton Apparatus for Structure and Spectroscopy) is a fixed target experiment at CERN dedicated to studies of the spin structure of the nucleon and of the spectroscopy of hadrons. During the years 2002-2004 and 2006-2007, the COMPASS collaboration has collected a large amount of data by scattering polarized 160 GeV/c muons on polarized <sup>6</sup>LiD and NH<sub>3</sub> targets. These data were used to evaluate the gluon contribution to the nucleon spin. The gluon polarization was directly measured from the cross-section helicity asymmetry of D<sup>0</sup> mesons production in the photon-gluon fusion reaction.

In 2008 COMPASS will perform a search for  $J^{PC}$ -exotic mesons, glueballs or hybrids, through light hadron spectroscopy in high energy (190 GeV/c  $\pi^-$ ) pion-proton reactions using both centrally produced and diffractive events. Preliminary results from diffractive pion dissociation into a  $\pi^- \pi^- \pi^+$  final state obtained in 2004 are also discussed.

## 1. THE COMPASS EXPERIMENT

The goal of the COMPASS experiment at CERN is to scrutinize how nucleons and other hadrons are built up from quarks and gluons. The main physics observables studied by the Collaboration are the polarisation of the constituents of a polarised nucleon, the mass and decay patterns of the light hadronic system with either exotic quantum numbers or strong gluonic excitation.

COMPASS takes advantage of a variety of high intensity beams (muons and hadrons) being located at the M2 beam line of CERN's Super Proton Synchrotron (SPS). The COMPASS setup was designed for the beams of 100 to 200 GeV/c and was built around two large dipole magnets, defining two consecutive spectrometers, covering a large and small scattering angles separately. To match the expected particle flux in the various locations along the spectrometer, COMPASS uses wide variety of very different tracking detectors: silicon detectors and scintillating fibers, Micromegas and GEM micromesh detectors, large proportional and drift chambers. Par-

ticle identification is performed using a RICH counter and both electromagnetic and hadron calorimeters. The polarized target (actually the largest polarized target in the world), consists of two oppositely polarized cells, 60 cm long each, surrounded by a large solenoid superconducting magnet. Until 2006, the two cells were filled with a <sup>6</sup>LiD target material (mainly deuterium), for which polarizations better than 50% are routinely achieved. In 2007 we are using ammonia (NH<sub>3</sub>, mainly proton), reaching polarizations of 90% and higher. Since 2006 a new target magnet has been used, increasing the acceptance from  $\pm 70$  mrad to  $\pm 180$  mrad. Also, the target material has been distributed in three cells, of 30, 60 and 30 cm length. A full description of the spectrometer can be found in [1].

Until 2008, the COMPASS collaboration has studied the spin structure of the nucleon via deep inelastic polarised muon-nucleon scattering. The 160 GeV polarised muon beam from SPS, with an intensity of  $2 \times 10^8$  muons per 4.8 s spill and a polarisation of  $\simeq 76\%$  is scattered off a polarised deuteron target. The target material, <sup>6</sup>LiD, has

been chosen for its high dilution factor (fraction of polarised nucleons  $f \simeq 40\%$ ). To reduce false asymmetries, the two target cells are polarised in opposite directions. The target polarization, of  $\simeq 50\%$ , is reversed once every 8 hours.

In 2008 COMPASS takes data with a hadron (composed of mainly  $\pi^-$  particles) beam. Several modifications were introduced in the COMPASS setup in order to adapt its capabilities to the constraints introduced by the hadron beam and by the hadron physics program requirements. These modifications are discussed in Section 3.2.

## 2. A “SPIN-CRISIS” AND THE GLUON POLARISATION MEASUREMENTS

Since 1988, when the EMC experiment found that only a small fraction of the nucleon spin is carried by the quarks,  $\Delta\Sigma = 12 \pm 9 \pm 14\%$  [2], the origin of the spin of the nucleon remains an intriguing puzzle. The discrepancy between this measurement and an expectation following from the relativistic quark models, which predict that 60% of the nucleon spin should come from the spin of quark and anti-quark constituents[3], was named “spin-crises”. The EMC result has been confirmed by series of deep inelastic scattering experiments at CERN, SLAC and DESY, giving, on average, a contribution from the quarks  $\Delta\Sigma$  to the nucleon spin is  $\sim 30\%$ .

The spin  $1/2$  of the nucleon can be decomposed as  $1/2 = 1/2\Delta\Sigma + \Delta G + L_{q+g}$  and one can conclude that the missing contribution to the nucleon spin must come from the gluons  $\Delta G$ , and/or from the orbital angular momenta  $L_{q+g}$ .

Here  $\Delta G$  is the first moment of the gluon helicity distribution  $\Delta g(x_g)$ . Experimentally, the polarisation  $\frac{\Delta g(x_g)}{g(x_g)}$ <sup>1</sup> of gluons carrying a fraction  $x_g$  of nucleon momentum is measured. The gluon polarisation can be directly measured via the spin asymmetry of the **Photon-Gluon Fusion** (PGF) process, shown in Fig. 1. The fragmenting  $q\bar{q}$  pairs are then detected with two different, but complementary methods.

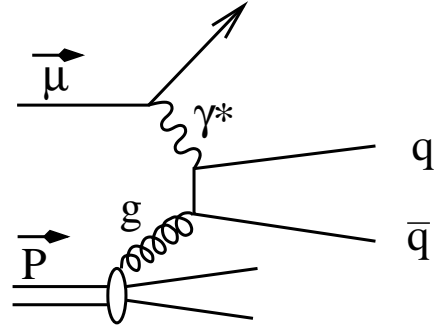


Figure 1. The photon gluon fusion process, used for direct measurements of the gluon polarisation. Fragmentation of the created  $q\bar{q}$  pairs into charmed D mesons gives a sample of events with minimal background for a  $\frac{\Delta g}{g}$  measurement.

In the first method (“open charm”[4]) the events where the charmed quark hadronises into a  $D^0$  or a  $D^*$  meson are selected. In the second one (low [5] and high  $Q^2$  [6] “high- $p_T$  pairs”), the PGF events are identified by requiring that two opposite-charge high-transverse momentum hadrons are detected in coincidence. Since this method selects light quarks as well, its counting rate is high; however, competing background processes play an important role introducing model dependence of its description. On the contrary the “open charm” leptonproduction method is clean, free from physics background but statistically limited.

Here we report results of the latest “open charm” analysis which includes the data collected between 2002 and 2006.

### 2.1. The $\langle \frac{\Delta g}{g} \rangle$ from “open charm” method

The cleanest way to tag the PGF reaction is the  $\gamma^* g \rightarrow c\bar{c}$  process because the presence of  $c$  quarks inside the nucleon is negligibly small. The created  $c\bar{c}$  pairs predominantly fragment into vector and pseudoscalar charmed-non-strange mesons in the following proportions  $D^*(2010)^\pm:D^*(2007)^0:D^\pm:D^0 = 3:3:1:1$ . All neutral and 68% of the charged vector

<sup>1</sup>Further instead of  $\frac{\Delta g(x_g)}{g(x_g)}$  a simplified notation as  $\frac{\Delta g}{g}$  will be used for gluon polarisation non averaged on  $x_g$  interval and  $\langle \frac{\Delta g}{g} \rangle$  for the averaged one.

mesons decay into the pseudoscalar  $D^0$  meson and the  $\pi^\pm$ ,  $\pi^0$  mesons or  $\gamma$ :  $D^*(2007)^0 \rightarrow D^0\pi^0, D^0\gamma$ ;  $D^*(2010)^\pm \rightarrow D^0\pi^\pm$ . Therefore, taking into account the  $D^0$  direct production and the cascade decays of vector mesons, the  $D^0$  mesons are produced more copiously than other weakly decaying D species.

The "open charm" analysis of the 2002-2006 data is based on the charged two-prong Cabibbo favoured  $D^0 \rightarrow K\pi$  decay channel with the branching ratio equals  $(3.80 \pm 0.09) \times 10^{-2}$ .

The separation of the primary and secondary  $D^0$  meson decay vertices is impossible due to multiple scattering in the thick polarised target, so an efficient particle identification with the RICH, even in low-multiplicity  $D^0$  decay modes, is crucial in such analysis. The constraint on mass difference  $\Delta M = M_{D^*} - M_{D^0}$  (so-called "D\* tag") was used for the effective combinatorial background suppression. In each event with  $D^0$  candidate the soft charged  $\pi$ -meson was searched for in order to detect the possible decay chain  $D^*(2010)^\pm \rightarrow D^0\pi^\pm$ . Finally two  $D^0$  samples were obtained (Fig. 2) with and without "D\* tag". The gluon polarization  $\frac{\Delta g}{g}$  is extracted from the measured double spin asymmetry  $A_{exp}$  of the  $D^0$  cross-section,

$$A_{exp} = P_B P_T f a_{LL} \frac{S}{S+B} \langle \frac{\Delta g}{g} \rangle \quad (1)$$

using the analysing power<sup>2</sup>  $a_{LL}$ , target polarisation  $P_T$ , beam polarisation  $P_B$ , dilution factor  $f$  and, finally, the signal purity  $\frac{S}{S+B}$ . As the "open charm" method is a statistically limited, a weighted method was developed to minimize the statistical error. In order to take into account the individual sensitivity of the selected events to  $\frac{\Delta g}{g}$  they were weighted as  $w = P_B f a_{LL} \frac{S}{S+B}$  [4].

The analysing power  $a_{LL}$  has to be determined from a Monte Carlo simulation, as the kinematics of the PGF event is not fully known because only one of the two charmed mesons is reconstructed. A parametrisation of  $a_{LL}$  was produced, using a neural network trained on a Monte Carlo sample

<sup>2</sup>The analysing power is defined as the ratio of spin-dependant and spin-ndependant photon-gluon cross-sections.

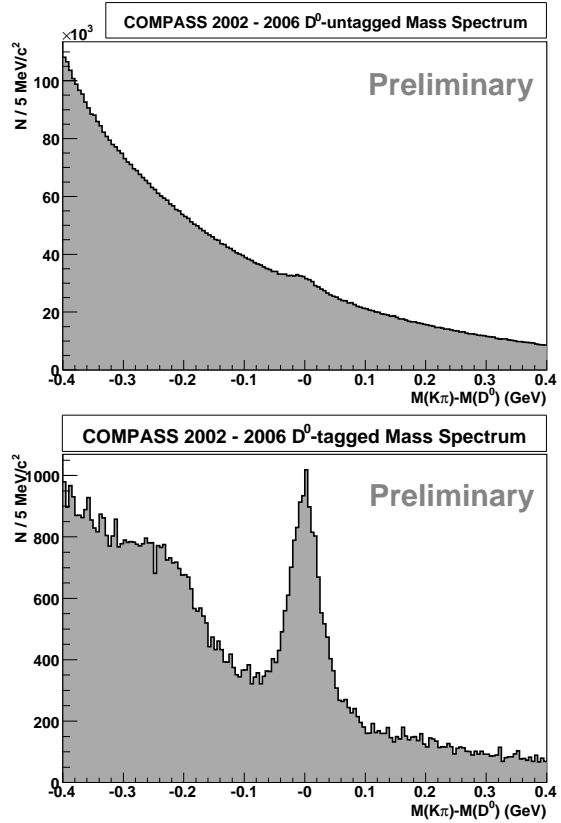


Figure 2. Invariant mass distributions of the  $D^0 \rightarrow K\pi$  candidates without (top) and with (bottom) "D\* tag".

generated by the AROMA generator and reconstructed as for the real data. A correlation of 82% is obtained between the parametrised and generated  $a_{LL}$ . The signal purity  $\frac{S}{S+B}$  parametrisation was built with Real Data taking into account the kinematics of the event, the RICH response and the invariant mass  $M(K\pi)$ [4]. This information provides a large range of variation for  $\frac{S}{S+B}$  resulting in a gain in statistics. A second advantage of this method is that the selection cuts can be relaxed sparing some signal events. The resulting gains in statistics are 15% and 45% for the  $D^0$  tagged and not tagged sample, respectively [4]. The statistical precision of the gluon polarisation

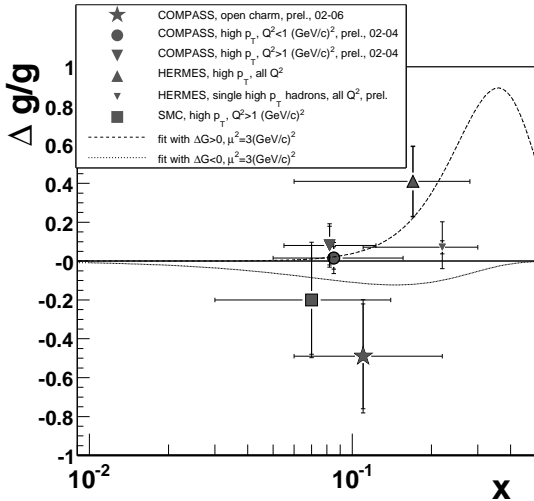


Figure 3. Comparison of direct gluon polarisation measurements obtained from open charm and high  $p_T$  hadron pairs analyses. The distribution of  $\frac{\Delta g}{g}$  at  $Q^2 = 3 \text{ (GeV/c)}^2$  for the QCD fits [9] with  $\Delta G > 0$  and  $\Delta G < 0$  are also shown.

measurement depends from the signal purity as follows  $\delta(\frac{\Delta g}{g}) \propto \frac{1}{\sqrt{\frac{S}{S+B} \times S}}$ .

Combining all 2002-2006 data a preliminary value of

$$\langle \frac{\Delta g}{g} \rangle = -0.49 \pm 0.27(\text{stat}) \pm 0.11(\text{syst.}) \quad (2)$$

corresponding to  $x_g = 0.11_{-0.05}^{+0.11}$  and a scale of  $\mu^2 \simeq 13 \text{ (GeV/c)}^2$  is obtained [4]. The largest contributions to the systematic uncertainty come from the parametrisation of  $a_{LL}$  and  $\frac{S}{S+B}$ .

## 2.2. Summary of the direct $\langle \frac{\Delta g}{g} \rangle$ measurements

The COMPASS results[4][5][6] are summarised in Fig. 3 and compared to previous measurements of SMC [7] and HERMES [8] experiments. The measurements indicate that  $\Delta G$  is small around  $x_g \sim 0.1$ .

In the same plot the distributions of  $\frac{\Delta g}{g}$  derived

from the QCD fits [9] are shown. The results of QCD analysis in the next to leading order (NLO) on all  $g_1(x)$  deep inelastic scattering data provide two solutions for the gluon spin distribution function  $\Delta G$ : one positive and one negative, as indicated by the two curves in Fig. 3. The two solutions describe the data equally well, so that no preference for any of the curves can be given so far. For both cases, at  $Q^2 = 3 \text{ (GeV/c)}^2$  the first moment of  $\Delta g$  is found to be small and in the range 0.2 – 0.3 in absolute value.

## 3. FUTURE HADRON PROGRAM

### 3.1. Introduction

Thirty-five years after the recognition that quark and gluons are the building blocks of matter, hadronic physics is at a turning point. The quark models of hadrons do not supply a realistic picture of the confinement of quarks and gluons in hadrons. A field theoretical based understanding is needed, in the framework of QCD. New theoretical tools have been developed and some experimental data have opened the way, but we are still lacking precise information on two central subjects: the spectroscopy of so-called exotic states, and the spatial structure of the nucleon. This is the context where, after several years of

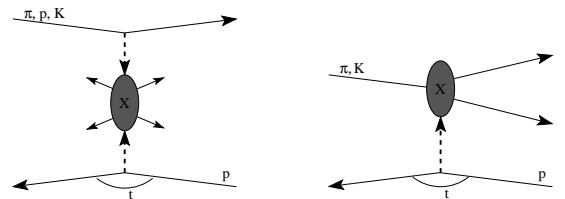


Figure 4. (left) Central production: large rapidity gap between scattered beam and produced particles; beam particle loses  $\sim 10\%$  of its energy; particles at large angles; possible source of glueballs. (right) Diffractive scattering: forward kinematics; large cross-section ( $\sim mb$ ); need to separate particles at very small angles; study of  $J^{PC}$ -exotic mesons.

running with a muon beam to study nucleon spin structure, the COMPASS collaboration is now preparing for the search for new exotic states, glueballs or hybrids, through light hadron spectroscopy in high energy pion-proton reactions, using both centrally produced and diffractive events (Fig. 4). QCD and derived models predict in particular the existence of  $q\bar{q}g$  hybrids, which are difficult to identify experimentally due to mixing with ordinary  $q\bar{q}$  mesons. However, some of them might have quantum numbers forbidden for  $q\bar{q}$  systems, e. g.  $J^{PC} = 0^{--}, 0^{+-}, 1^{-+}$ . Their observation would therefore provide a fundamental confirmation of QCD.

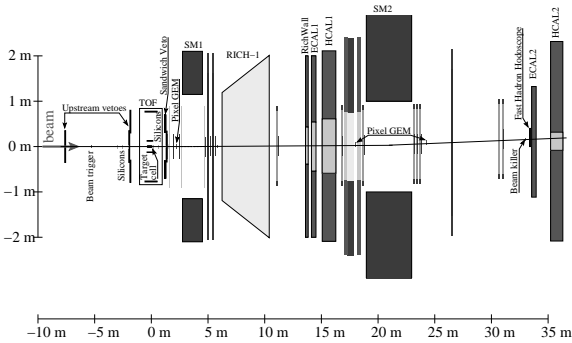


Figure 5. Schematic view of the COMPASS layout for the hadron beam.

### 3.2. Spectrometer in the 2008 hadron run

For the run with a hadron beam, several major modifications of the COMPASS setup were made. The polarised target was substituted by a liquid hydrogen target with a cell of 40 cm length and 3.5 cm diameter, surrounded by a Time-of-Flight (ToF) system, as shown in Fig. 5. To the existing upstream silicon telescope, a downstream telescope was added, in order to precisely measure the direction of secondary particles produced in the target.

A big effort has been dedicated to minimise the amount of material along the beam path and

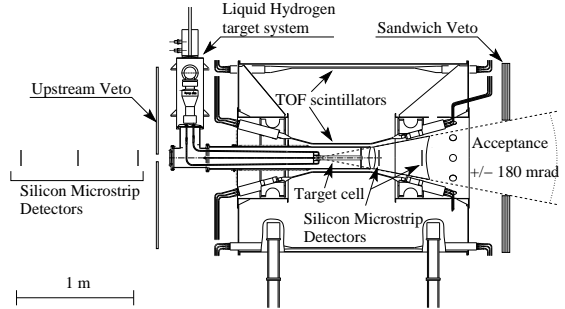


Figure 6. Target region showing: - the upstream silicon micro-strip tracker, - the liquid hydrogen target, - the inner and outer ToF scintillator rings, - the downstream silicon micro-strip tracker.

in the region close to it, thus reducing the background from secondary interactions. New GEM detectors, with a pixelised readout in the central region, have been developed [10] and used for a replacement of several of the scintillating fibre detectors tracking the particles at very small angles. A position resolution of  $90 \mu\text{m}$  and timing resolution of 8 ns were reached.

The slow recoil proton produced at large angle in central production and diffractive projectile excitation is detected by the Recoil Proton Detector (RPD) which surrounds the liquid hydrogen target, as shown in Fig. 6. The RPD is made of an inner ring and an outer ring of scintillator counters equipped with PMs fixed to a cylindrical support structure. The Monte Carlo momentum distribution of detected recoil protons produced in the diffractive pion-proton scattering shows that the momentum cutoff is at about 290 MeV/c, corresponding to a squared four momentum transfer  $-t > 0.06 (GeV/c)^2$ .

In 2008 COMPASS is collecting data from two production mechanisms using  $\pi$ , K and p projectiles. The compositions of 190 GeV hadrons beams are following - 96%  $\pi$ , 3.5% K, 0.5% p - negative beam and -75% K, 25%  $\pi$  the positive one. The beam intensity is  $5 \times 10^6 \text{ had/s}$  and the corresponding luminosity is  $0.15 \text{ pb}^{-1}/\text{day}$

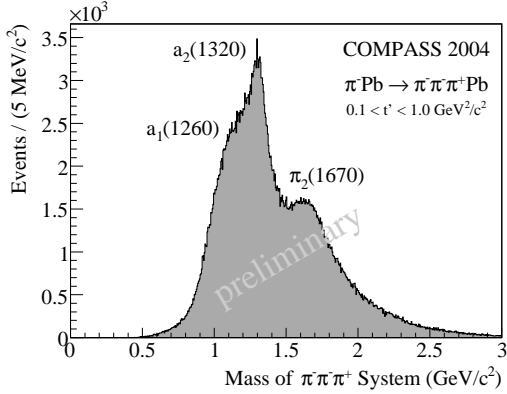


Figure 7. The invariant mass  $\pi^- \pi^- \pi^+$  final state for  $0.1 < t' < 1.0$  ( $GeV/c^2$ ). In this kinematic domain of large four momentum transfer the scattering on nucleons is dominating. Well-known  $a_1(1260)$ ,  $a_2(1320)$  and  $\pi_2(1670)$  states come out correctly

In diffractive scattering is planned to recorder during  $\sim 35$  days about  $1.6 \times 10^5$   $\pi_1(1600)$  events:  $\pi^- p \rightarrow \pi_1(1600)p$ ,  $\pi_1(1600) \rightarrow \pi^- \pi^- \pi^+$ .

During the 60 days is expected to recorder  $\sim 2 \times 10^3$   $f_0(1500) \rightarrow \eta\eta \rightarrow 4\gamma$  and  $\sim 1 \times 10^5$   $f_0(1500) \rightarrow 2\pi^- 2\pi^+$  decays in the central production reaction  $\pi^- p \rightarrow \pi^- f_0(1500)p$ .

### 3.3. 2004 hadron pilot run and diffractive dissociation

Diffractive dissociation reaction<sup>3</sup>  $\pi^- Pb \rightarrow \pi^- \pi^- \pi^+$  in COMPASS using a 190 GeV/c  $\pi^-$  beam provide clean access to meson resonances with masses below 2.5  $GeV/c^2$ . In this mass region the candidates for spin-exotic states  $1^{-+}$  hybrid, the  $\pi_1(1600)$ , was observed in diffractive production and decaying to  $\rho\pi^-$  [11]. During the 2004 pilot hadron run, a competitive number of events taken with a lead target were recorded within a few days of data taking. Primary vertices with one incoming negative and three out-

<sup>3</sup>In 2004 hadron run a Primakoff scattering was the main aim, thus a lead target was chosen. A dedicated trigger was set up to study diffractive production also.

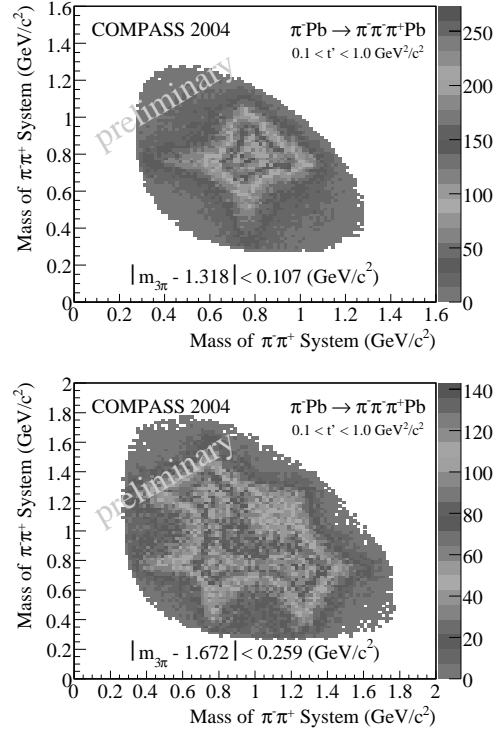


Figure 8. Dalitz plots for  $a_2(1320)$  (*top*) and for  $\pi_2(1670)$  (*bottom*), selected by a  $\pm 1\Gamma$  cut around its nominal mass. The dominant decays  $a_2 \rightarrow \rho\pi$  and  $\pi_2 \rightarrow \rho\pi$ ,  $f_2\pi$  are clearly visible.

going ( $-$ ,  $-$ ,  $+$ ) particles are required. An exclusivity cut ensures that, taking into account also the momentum transfer  $t' = |t| - |t|_{min}$  to the target, the total energy of the three outgoing pions sums up to the beam energy. COMPASS has an excellent acceptance for diffractively produced  $3\pi$  events, which is of the order of (55 – 60)% The final event sample comprises about 420 000 events in the interval  $0.1 < t' < 1.0$  ( $GeV/c^2$ ). Fig. 7 presents their invariant  $3\pi$  mass spectrum, which represents the dominantly produced mesons  $a_1(1260)$ ,  $a_2(1320)$  and  $\pi_2(1670)$ . In Fig. 8 the (non-squared) Dalitz plots for the  $a_2(1320)$  and  $\pi_2(1670)$  mass regions are shown.

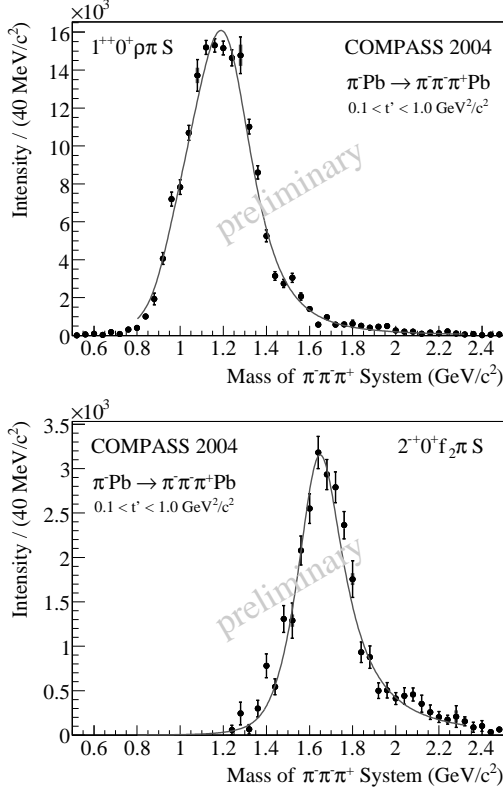


Figure 9. (*top*) Intensity of the  $1^{++}0^+[\rho\pi]S$  wave corresponding to the production of the  $a_1(1260)$  meson. (*bottom*) Intensity of the  $2^{-+}0^+[f_2\pi]S$  wave corresponding to the production of the  $\pi_2(1670)$  meson.

### 3.4. Partial Wave Analysis (PWA) results

The PWA is based on the isobar model and the Zemach formalism. One partial wave is characterized by a set of quantum numbers  $J^{PC}M^\epsilon[isobar]L$ , where  $J^{PC}$  represents the spin, parity and C-parity of the resonance X, respectively. M and  $\epsilon$  (reflectivity) describe the spin projection. X is assumed to decay into a di-pion  $[isobar]$  and a bachelor  $\pi^-$ , which have a relative orbital angular momentum L. The *isobar* further decays into a  $\pi^+\pi^-$  pair. The PWA is divided into two steps, namely a mass independent

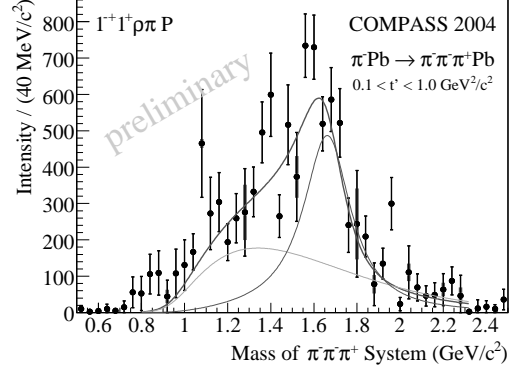


Figure 10. The spin-exotic  $1^{-+}1^+[\rho\pi]P$  wave corresponding to the production of the  $\pi_1(1600)$  hybrid candidate. A background (*purple*) and a BW function (*blue*) have been used in the mass dependent fit to describe this partial wave.

and a For the subsequent mass dependent fit a subset of seven waves has been selected:  $0^{-+}0^+[f_0(980)\pi]S$ ,  $1^{-+}1^+[\rho\pi]P$  (spin-exotic),  $1^{++}0^+[\rho\pi]S$ ,  $2^{-+}0^+[f_2\pi]S$ ,  $2^{-+}0^+[f_2\pi]D$ ,  $2^{++}1^+[\rho\pi]D$  and  $4^{++}1^+[\rho\pi]G$ . The intensities and interferences of these waves are parameterized with relativistic **Breit-Wigner** (BW) and eventually background functions. From this fit, which is shown as red curve overlaid to the mass independent fit results, resonance masses and widths have been obtained.

In Fig. 9 the intensity of the two dominant partial waves in the mass dependent fit is presented. The Fig. 10 shows the spin-exotic  $1^{-+}$   $\pi_1(1600)$  signal. The mass-dependent fit gives the values of the mass and width of  $1.660^{+0.010}_{-0.074}$  and  $0.269^{+0.063}_{-0.085}$   $\text{GeV}/c^2$  respectively which is consistent with the hybrid candidate  $\pi_1(1600)$  [11].

The preliminary values of BW parameters of all fitted resonances are presented in Table 1. The well known states of  $a_1(1260)$ ,  $a_2(1320)$  and  $\pi_2(1670)$  are well resolved confirming the PDG values for mass and width with high quality. In addition, we observe states not yet established in the PDG like  $\pi_1(1600)$ , as well as hints for the

Table 1  
Preliminary results from mass-dependent fit compared to PDG values

State	Mass&Width	COMPASS $\pm$ stat $\pm$ syst ( $GeV/c^2$ )	PDG ( $GeV/c^2$ )
$a_1(1260)$	M	$1.256 \pm 0.006 + 0.007 - 0.017$	$1.230 \pm 0.040$
	$\Gamma$	$0.366 \pm 0.009 + 0.028 - 0.025$	0.250 to 0.600
$a_2(1320)$	M	$1.321 \pm 0.001 + 0.000 - 0.007$	$1.3183 \pm 0.0006$
	$\Gamma$	$0.110 \pm 0.002 + 0.002 - 0.015$	$0.107 \pm 0.005$
$\pi_1(1600)$	M	$1.660 \pm 0.010 + 0.000 - 0.064$	$1.653+0.018-0.015$
	$\Gamma$	$0.269 \pm 0.021 + 0.042 - 0.064$	$0.225+0.045 -0.028$
$\pi_3(1670)$	M	$1.659 \pm 0.003 + 0.024 - 0.008$	$1.6724 \pm 0.0032$
	$\Gamma$	$0.271 \pm 0.009 + 0.022 - 0.024$	$0.259 \pm 0.009$
$\pi_1(1800)$	M	$1.785 \pm 0.009 + 0.012 - 0.006$	$1.812 \pm 0.014$
	$\Gamma$	$0.208 \pm 0.022 + 0.020 - 0.037$	$0.207 \pm 0.013$
$a_4(2040)$	M	$1.884 \pm 0.013 + 0.050 - 0.002$	$2.001 \pm 0.010$
	$\Gamma$	$0.295 \pm 0.024 + 0.046 - 0.019$	$0.313 \pm 0.031$

known state  $a_4(2040)$ . Remarkably we observe the well established  $\pi_1(1800)$  despite being a very small signal as it is produced preferably at small momentum transfers to be analyzed later. mass dependent fit [12].

#### 4. Conclusion and outlook

In summary, all COMPASS results for gluon polarisation measurements performed on data taken in 2002-2006 indicate a small value of  $\Delta G$ . Similarly, the QCD analysis of  $g_1$  data also indicates a small value of the first moment of  $\Delta g$ . These results are the probable signature for a predominant role of the angular orbital momentum in nucleon spin decomposition in the frame of the parton model and perturbative QCD.

The data taking continues in 2008 with a spectrometer modified for hadron spectroscopy studies. The first goal in the diffractive scattering will be a further investigation of the hybrid candidate  $\pi_1(1600)$ . In the central production the efforts will be put to glueball candidate  $f_0(1500)$ .

The PWA analysis of the diffractive meson production obtained in the 2004 preliminary hadron run shows that the well-known  $a_1(1260)$ ,  $a_2(1320)$  and  $\pi_2(1670)$  states are correctly measured. Moreover, this analysis shows a clear signal for the still controversial spin-exotic  $\pi_1(1600)$  meson.

#### REFERENCES

1. P.Abbon et al.,Nucl.Instr. Meth. A577 (2007) 455.
2. J. Ashman *et al.*, Phys. Lett. B206 (1988) 364.
3. J. Ellis and R.L.Jaffe, Phys. Rev. D9 (1974) 444, Phys. Rev. D10 (1974) 1669.
4. F. Robinet, Proc. of the 16th Int. Workshop on Deep Inelastic Scattering, London, England (2008).
5. E.S. Ageev *et al.*, Phys. Lett. B633 (2006) 25.
6. M. Stolarski, Proc. of the 16th Int. Workshop on Deep Inelastic Scattering, London, England (2008).
7. B. Adeva *et al.*, Phys. Rev. B70 (2004) 012002.
8. A. Airapetian *et al.*, Phys. Rev. Lett. 84 (2000) 2584.
9. Yu.V.Alexakhin *et al.* Phys. Lett. B647 8 (2007).
10. T.Nagel, Proc. of the 10th ICATPP Conference, Como. Italy (2007).
11. S. U. Chung et al., Phys. Rev. D65, 072001 (2002); A. R. Dzierba et al., Phys. Rev. D73, 072001 (2006);Y. Khokhlov, Nucl. Phys. A663, 596 (2000).
12. Q.Weitzel, Proc. of the 10th Int. Workshop on Meson Production, Krakow, Poland (2008).